Technical Note

Importance of mode detection in ambient noise array application for shear wave velocity profile determination

M. fazlavi[1], E. Haghshenas[2,*]

Abstract

In this paper we are going to show the importance of mode identification in microtremor array analysis. The idea come from four concentric ambient noise array recordings with aperture 100 to 1000 meters, performed in southern urban area of Tehran near the shrine of Imam Khomeini. These measurements were part of a comprehensive research project with the aim of determination of deep shear wave velocity model of Tehran alluvial deposits. Using appropriate signal processing techniques, including array processing methods as well as classical and time-frequency horizontal/vertical spectral ratio, the dispersion curves of surface waves, fundamental resonance frequency and Ellipticity of Rayleigh waves, were extracted. In the final step, the shear wave velocity profile of the site was determined by joint inversion of all of these attributes. The results show 2 different energetic trends in dispersion curves, for arrays of aperture 200 and 400 meters that one of them is coincide with 100m aperture array. For array with aperture 1000m any clear trend of energy could be observed because of deficiency of energy in low frequency. The inversion of data obtained by 100m aperture array alone, assuming the dispersion curve as fundamental mode (a common procedure in urban area) result in shear wave velocity that is not match with existing geological information. Performing the inversion, assuming 2 energetic trends, observed for larger arrays; one as fundamental mode and another as mode 1 of Rayleigh waves, can modify significantly the shear wave velocity profile in accordance with existing geological and geotechnical information. This study show the importance of extracting of correct dispersion curves with detecting fundamental and higher modes, using array measurement with various aperture at one place to obtain more realistic shear wave velocity profile.

Keywords: Shear wave velocity, Microtremor array, Higher modes effect.

1. Introduction

Recently, some microtremor array study performed in south of Tehran (Davoodi et al, 2008 and 2009 and Shabani et al, 2008) in order to extracting the shear wave velocity profile of soil. Due to their small aperture arrays (less than 100 meters), they failed to estimate the shear wave velocity deeper than 150 meters [1, 2, 3]. Shabani in 2008 proposed bedrock depth between 700 to 1200 meters for south of Tehran (near Park Velayat), using inversion of dispersion curves as well as transfer function calculation. On the other hands, some other studies (Mottaghi et al, 2012, Norouzi, 2013, Shirzad et al, 2013) using tomography technique based on cross correlation of earthquake or microtremor data, tried to estimate average shear wave velocity profiles

in some section across the city [4, 5, 6]. However, regarding the distance between pair of stations used in these studies, accuracy and resolution of shear wave velocity profile are reliable only for the depths greater than 1 km.

Reviewing all of previous array studies in southern parts of Tehran, proposed us two probable reasons, that can explained why these studies failed to estimate deep velocity profile; 1) their small array aperture and 2) the lack of microtremor energy especially in low frequency in Tehran region.

From 2012, a series of multi array microtremor measurement in 11 locations have been conducted by IIEES (International Institute of Earthquake Engineering and Seismology) in the framework of a research project [7, 8]. These measurements have been arranged in two sections with north-south and east-west direction (**Fig. 1**).The goal of this project is to get a comprehensive view of seismic behavior of Tehran substructure, and investigation of shear wave velocity of thick alluvial deposits above the geological bedrock. The large arrays (up to 1000 meter diameter in some locations) were used; depend on assumed bedrock depth based on geological

* Corresponding author: hagshen@iiees.ac.ir
1 Ph.D Candidate, International Institute of Earthquake Engineering and Seismology
2 Ph.D, International Institute of Earthquake Engineering and Seismology

perspectives. For an exhaustive interpretation of the results, joint inversion of ellipticity and dispersion properties of Rayleigh waves, combined with known geotechnical and surface geophysical data and earthquake HVSR (horizontal to vertical spectral ratio) peaks were applied. Fig. 2 shows how this various information was used and compiled to cover a wide range of frequencies, necessary to obtain a relatively complete profile of shear wave velocity.
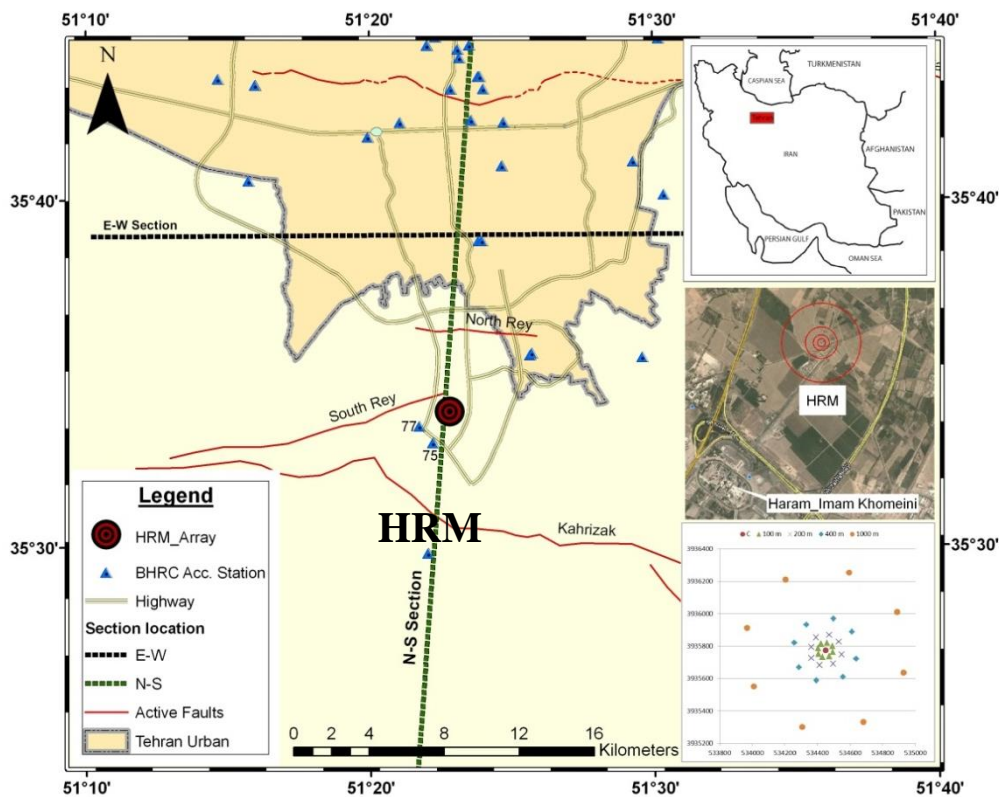

Fig. 1 Location of study area in south of Tehran, marked as HRM. Panels on right hand of the figure show configuration of 4 recorded arrays using 8 seismological sensors with apertures 100-200-400 and 1000 meters that have been measured in different days
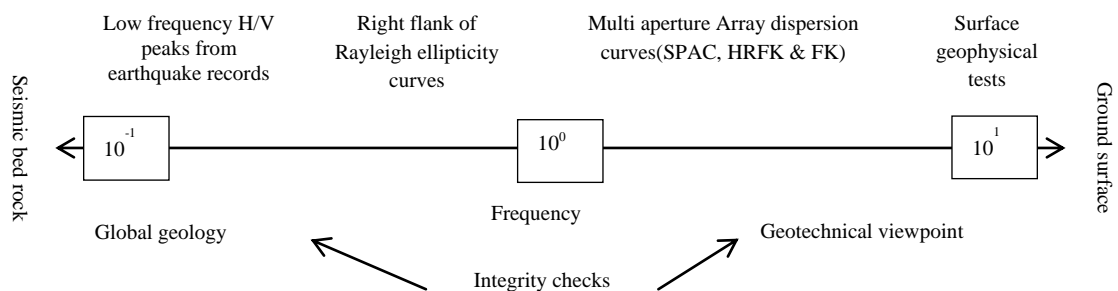

Fig. 2 general idea to deep alluvium of Tehran investigation methodology (Fazlavi et al, 2014)

Usually the observed dispersion curves from an array measurement are interpreted as fundamental mode of Rayleigh wave in inversion processing, while they could be a higher modes. This paper focuses on the effect of consideration of higher modes in inversion analysis. For this purpose an array in south part of the study area presented by HRM on the Fig. 1 is considered. The extracted dispersion curves shows two distinguish high energy trend considering the collective dispersion curves (dispersion curves obtained from small to large aperture arrays) and assumption of the higher mode result in more realistic shear wave profile.

2. Microtremor and Geotechnical Data Acquisition

HRM array located on 534418 and 3935718 based on UTM coordination (Fig. 1a). We arranged 4 concentric circular arrays with aperture 100, 200, 400 and 1000 meter in 4 different days. For each array, we used 8 three component seismographs (CMG-6TD velocimeter) regularly on circumference as well as 1 station at the center of array (Fig. 1b). Measurement duration was 1 to 3

hours simultaneously for all stations and the absolute time were provided by connecting GPS. We use Butterworth filtering between 0.2 to 20 Hz for all the data consistent with constant part of instrumental response and phase of applied velocimeters.

In addition to these measured data we also used some earthquake data recorded by two accelerometeric stations belong to ISMN (Iran Strong Motion Network), installed by BHRC (Building and Housing Research Center). These two stations, type of Guralp CMG5, are installed at shrine of Imam Khomeini near HRM location and recorded some major earthquakes occurred since 2000.

Based on some existing boreholes data, drilled down to 25 meters, during a bridge construction project in the studied area, the soil profile consist of fine grain materials (ML or CL in USCS classification). SPT (Standard Penetration Test) numbers vary between 20 to 40 which is equivalent to shear wave velocity between 350 to 430 m/s based on experimental SPT-Vs relationship (Equation 1), given by JICA for this type of soils in Tehran [9] (see detailed data in Table and Fig. 3).

$$V_s(m/s) = 161 \times SPT^{0.277} \tag{1}$$

Table 1 Geotechnical data (estimated shear wave velocity based on SPT and soil classification) from 4 boreholes drilled north of HRM measured array (UTM coordination 535477 and 3937721)

| DEPTH	BH05			BH06			BH07			BH08		
(m)	SPT	Vs (m/s)	Clas.	SPT	Vs (m/s)	Clas.	SPT	Vs (m/s)	Clas.	SPT	Vs (m/s)	Clas.
2	29	409		14	334		14	334		14	334	
4.00	33	424	CL	37	438	ML	25	393	CL	30	413	
6.00	19	364		29	409	CL	15	341		35	431	ML
8.00	--			--			31	417		19	364	
10.00	26	397		24	388		14	334		15	341	CL
12	31	417	ML	14	334	ML	--			11	313	
14.00	38	441		23	384	CL	41	450	ML	--		ML
16.00	--			63	507		16	347	CL	25	393	
18.00	35	431		41	450		--			27	401	CL
20.00	33	424		38	441	ML	25	393		33	424	
22	--			--			28	405	ML	--		ML
24.00	42	453		39	444	CL	24	388		41	450	
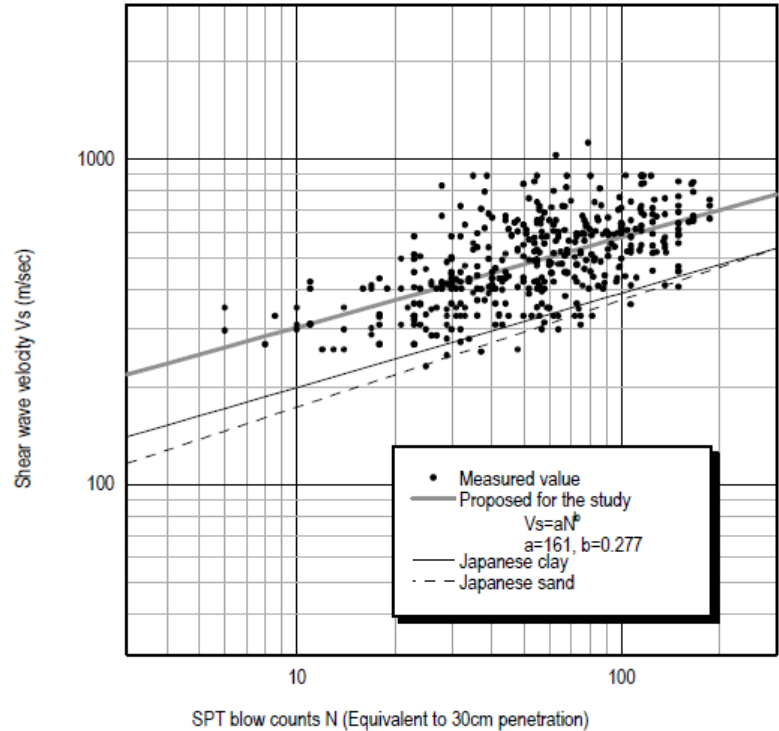
Fig. 3 The relationship of SPT and Shear wave velocity for Tehran soils based on JICA (2000) evaluation report. Thick gray line indicates best fit line for Tehran compared with Japanese soil formula shown by dash and thin lines

3. Data Analysis

According to mentioned strategy (Fig. 2) in order to cover wide frequency bands by observed data, especially regarding the low energy of microtremor for the frequencies smaller than 1 Hz, 4 step of analysis are considered; step 1: calculation of dispersion curves by array processing of 4 concentric array measurements, step 2: determination of fundamental resonance frequency of the site, using horizontal/vertical spectral ratios of earthquake data of ISMN stations and ambient noise recoded during this study, step 3: extracting ellipticity curves from ambient noise recorded by 36 stations during array measurements, Step4: joint inversion of all the above mentioned parameters, obtained from 3 previous steps, in order to extracted best model of shear wave velocity (see Fig. 4). In addition, verification processing were considered and theoretical dispersion and ellipticity curves are recalculated based on the back analysis of obtained best model.

All the processing steps have been performed using Geopsy software packages provided by the SESAME consortium.
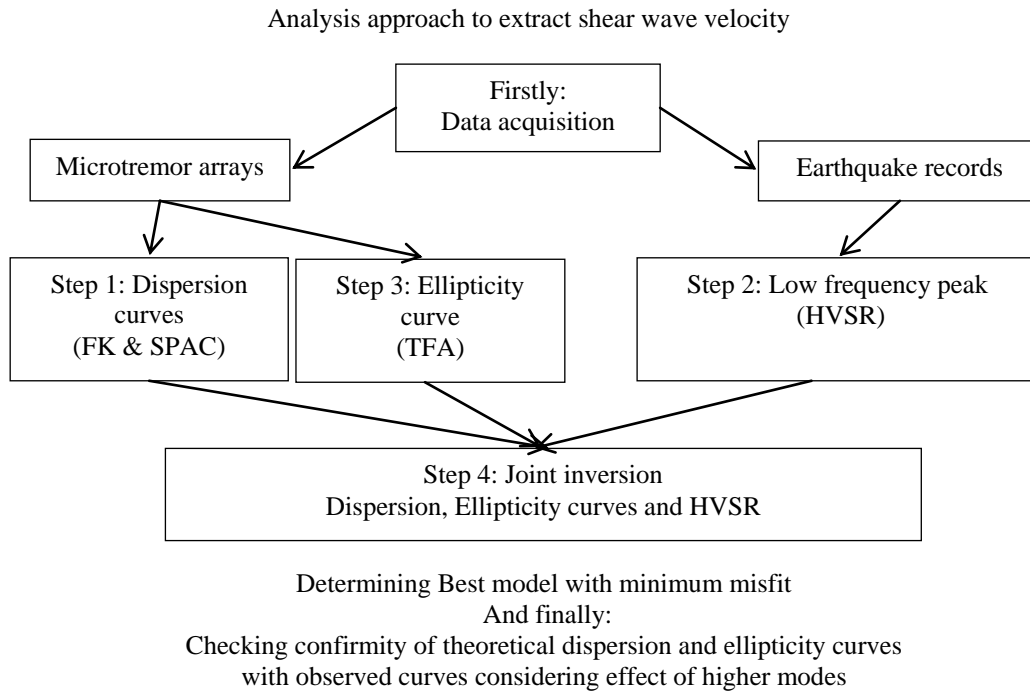
Analysis approach to extract shear wave velocity

Fig. 4 diagram of approach of microtremor array analysis for determining shear wave velocity

3.1. Step 1: extracting dispersion curves by array processing

Dispersion property of surface wave is a base of array microtremor measurement methods, Frequency-Wave number (F-K) and Spatial Autocorrelation coefficient (SPAC). Generally, these array processing methods are performed only applying vertical component of ambient noise recordings using dispersion property of Rayleigh waves. Since penetration depth of surface wave depend to frequency, shear wave velocity (Vs) profile can be driven from inverting of dispersion curve. But due to contribution of different modes of surface wave, estimated shear wave velocity is not unique [10].

To selecting valid parts on dispersion curves, Tokimatsu (1997) presented the following relationship between the inter-station distances and the desired wavelengths that can be used in array measurement design [11].

$$2D_{min} < \lambda_{min} < \lambda_{max} < 3D_{max} \qquad (2)$$

D_{min} and D_{max} is minimum and maximum inter-station distance, λ_{min} is minimum wavelength to avoid the aliasing error and λ_{max} is maximum valid wavelength less than 3time D_{max}, due to site filtering effect. Considering $k=2\pi/\lambda$, valid ranges of wavenumber intervals for the measured arrays, Kmax and Kmin are equal 0.1 and 0.0014 m^{-1}, respectively from smallest to largest inter-station distances.

Frequency-Wavenumber (FK) method was used in order to calculate dispersion curves. This method introduced first by Locass and capon in 1969, Asten and Henstridge, 1984 and described recently by Okada in 2004 base on power density of correlation of signals transferred between two stations [12, 13, 14, 15]. For calculating the frequency–wavenumber power spectral density, using Limited Fourier Transform, firstly the cross correlation functions $S(\Delta x, \Delta y, \tau)$ should be estimated as Equation 3.

$$S(\Delta x, \Delta y, \tau) = E[X^*(x_j, y_j, t_j)X(x_i, y_i, t_i)] \qquad (3)$$

Where, $\Delta x = x_i - x_j = r\cos\theta$, $\Delta y = y_i - y_j = r\sin\theta$ and $\tau = t_i - t_j$. The array output (phase velocity dispersion curve) is normalized dividing by the maximum spectral power which is called the semblance parameter. Using maximum of wave number semblance (K_0) in the wave-number planes (K_x, K_y) at specified frequency (ω_0), the phase velocity (C_0) of the traveling waves across the array can be estimated by equation 4.

$$C_0 = \frac{\omega_0}{k_0} = \frac{2\pi f_0}{\sqrt{k_{x0}^2 + k_{y0}^2}} \tag{4}$$

Fig. 5 shows individual phase velocity dispersion curves for all arrays with aperture 100, 200, 400 and 1000 meters. The clear high energy trends can be observed for smaller arrays, especially array of 100m aperture, while for large array any distinguish trend is revealed, because of deficiency of energy of ambient noise at their valid frequency ranges. Considering the dispersion curves of different recorded array all together, a good overlap covering a relatively wide frequency range can be seen in

Fig. 5, however there is a clear shift in trend of dispersion curves between frequencies 3 to 4 Hz.

In addition to F-K method, we used Spatial Autocorrelation Coefficient (SPAC) method presented originally by Aki in 1957. Henstridge (1979) developed relationship between Spatial Autocorrelation Coefficient and phase velocity of fundamental mode of Rayleigh waves [16, 17]. This method modified by Bettig in 2001 using correlation concept between vertical components of recorded noise at each pair of stations, keeping same azimuth especially at the irregular and large aperture array in urban area [18].

Bottom right panel of Fig. 5, shows dispersion curves related to autocorrelation curves of SPAC analysis obtained using Bettig approach. Although like F-K results, some trends of higher modes could be seen on SPAC dispersion curves, however normally these parts of dispersion curves in SPAC method are considered as unreliable parts that should be ignored. As can be seen on this figure, there is a good agreement of averaged collective FK dispersion curves and SPAC outputs at fundamental mode.
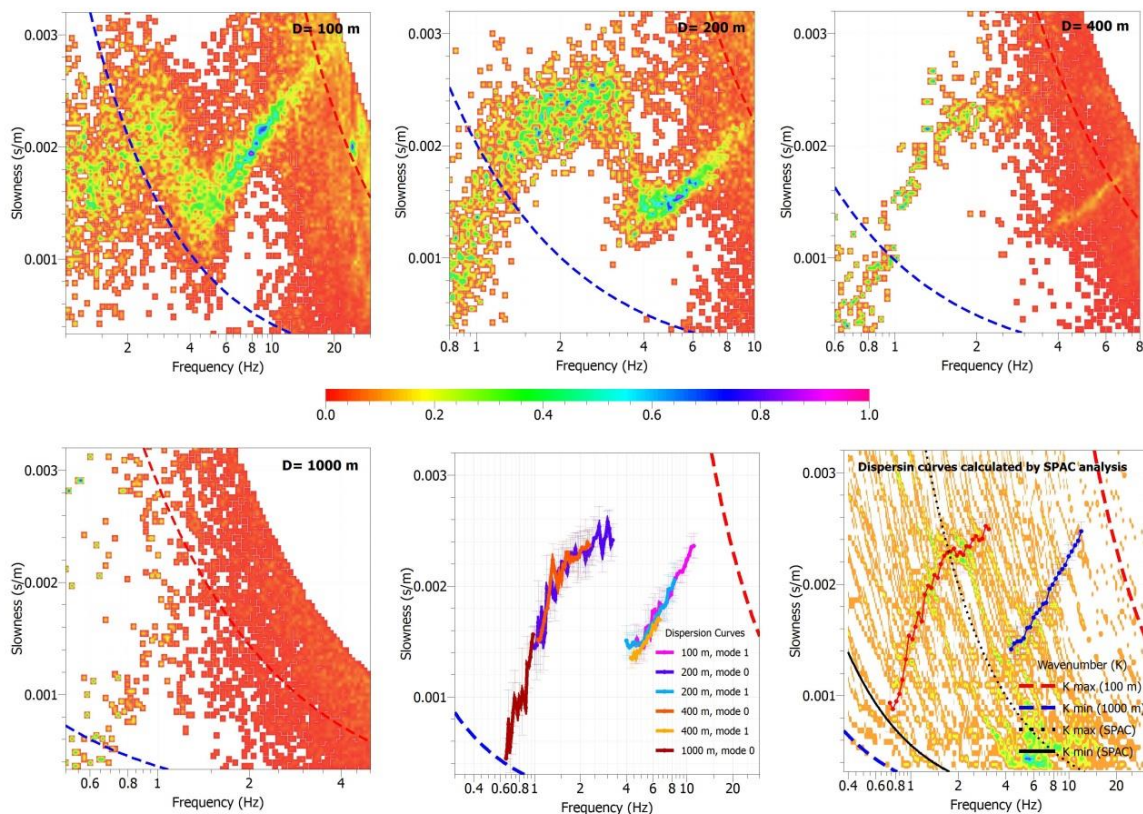

Fig. 5 dispersion curves for all arrays in HRM station. Fundamental and higher modes could be observed on large to small aperture arrays. Also compatibility of FK and SPAC dispersion curves would be shown on bottom-right shape

3.2. Step 2: calculating fundamental resonance frequency using classical HVSR

The fundamental resonance frequency (f_0) of a site is an indicator for depth of contrast between the alluvial deposit and bedrock and can be used as one of the input parameters in joint inversion processing. One of the well

known techniques for determination of this frequency is HVSR (Horizontal to Vertical Spectral Ratio) technique based on dividing quadratic averaged or total energy of horizontal components by vertical component. This technique was proposed originally by Nogshi and Igarashi in 1970 and then became popular by Nakamora in 1989 [19]. The main usage of HVSR technique is to extract peak

frequency of HV curves, which is compatible with fundamental Resonance frequency (f_0) of soil alluvium [11, 20, 21, 22]. HVSR is applicable on both ambient noise and earthquake records and many experimental comparison show compatibility of the results between these two categories of data [22, 23].

To calculate the H/V ratio on microtremor data, after necessary waveform operation such as offset removal and band pass filtering, stationary windows was selected to avoid transient signals using the anti-triggering algorithm provided in Geopsy package with STA/LTA threshold (0.3 to 2.0). The length of the windows was determined at 40 to 60 sec with 5% cosine tapering. Spectral amplitudes using FFT and Konno and Ohmachi smoothing (b= 20 to 40%) were calculated for the three components (E, N & Z).

One of the problem, using HVSR on ambient noise data, in Tehran is the lack of microtremor energy on low frequency signal (0.1-1 Hz), because of the distance between Tehran and oceans (the nearest sea to Tehran is Caspian Sea with a distance about 100 Km) as the source of the ambient noises in these range of frequencies [24, 25]. In order to overcome this deficiency of energy we also calculate horizontal/vertical spectral ratio using earthquake records. These records have a sufficient energy to excite the deep bedrock contrast of Tehran. For this purpose an earthquake event, occurred on 2009, near to Rey at south of Tehran, recorded by stations 75 and 77 of ISMN near HRM [26] was used. To calculate H/V on earthquake records, only coda part of record (usually has window length less than 20 to 30 S) with cosine taper 5 to 10% and Konno and Ohmachi smoothing (b= 20 %) was considered. The H/V curve obtained from both of earthquake event and ambient noise (averaged for all 36 station installed during array measurements) show a clear peak at 0.65± 0.1 (Fig. 7) that is indication of a deep seismic contrast for this site.

3.3. Step 3: calculating ellipticity of rayleigh waves using HVTFA technique

Many researchers had been shown that the H/V peak coincides with maxima at ellipticity curve of surface waves. For example, Fah et al. (2001) showed that there is generally a good agreement between H/V ratios and the theoretical ellipticity curves of the fundamental-mode of Rayleigh wave close to the fundamental resonance frequency of the site as the right flank of curve [27]. This part of Ellipticity curve is detectable in Horizontal to vertical spectral ratios of Rayleigh wave between the peak at the fundamental resonance frequency and the first minimum at higher frequency. So the HVSR technique is used as well for extracting the Ellipticity of surface wave. If contribution of the love and body waves can be omitted, only ellipticity of Rayleigh wave would be remained on HVSR curves. With this purpose, to calculate Ellipticity, we used the Time-Frequency Analyzing (TFA) method based on the modified Morlet wavelet as described in NIRIES-D4, 2010 [28]. The relation for spectral representation of the modified Morlet wavelet is presented as equation 5:

$$\Psi(\omega) = \frac{1}{\sqrt[4]{\pi}}\exp(-m(a\omega - \omega_0)^2), \quad for\ \omega > 0 \qquad (5)$$

Where parameter m controls the wavelet's width in the spectral domain and ω_0 is central angular frequency of the modified Morlet wavelet at a=1. The higher value of parameter m, the narrower is the wavelet in the spectral domain, the frequency resolution is improved but the time resolution is reduced. The choice m= 1/2 corresponds to the original Morlet wavelet (See NIRIES-D4, 2010, for detail time domain Morlet formulation as a common choice of the wavelet analysis for continuous wavelet transform [CWT]). Ellipticity is estimated from the average (geometrical mean) of the histogram values (the probability density function, PDF) for a certain frequency. In the time-frequency method of H/V computation, the H/V ratio is not computed from the whole spectra for vertical and horizontal components of the ambient noise as in the classical HVSR method. Only parts of the histogram, correspond to the highest values of the PDF, are influenced by the Rayleigh wave contribution. Other parts of the histogram may be influenced by contributions from other waves (love or body waves) on the horizontal component with frequency content and arrival times similar to those of Rayleigh waves on the vertical component. These other waves can only be partly separated out by the wavelet method. On the other hands, NPPM parameter (number of maxima used per minute) was defined to reduce the influence of a single time window and to use energy maxima well distributed over the signal. Using small values of NPPM, makes the selection more rigorous (only the most energetic time-frequency maxima per minute are used for the histogram computation).

In this study, after checking different number for m and NPPM parameters, finally we selected m=5 and NPPM=2 for all stationary microtremor data. Selection of the best parameters in this method needs a lot of computing with different numbers in each station. Fig. 6 shows averaged ellipticity curve of all 36 stations.
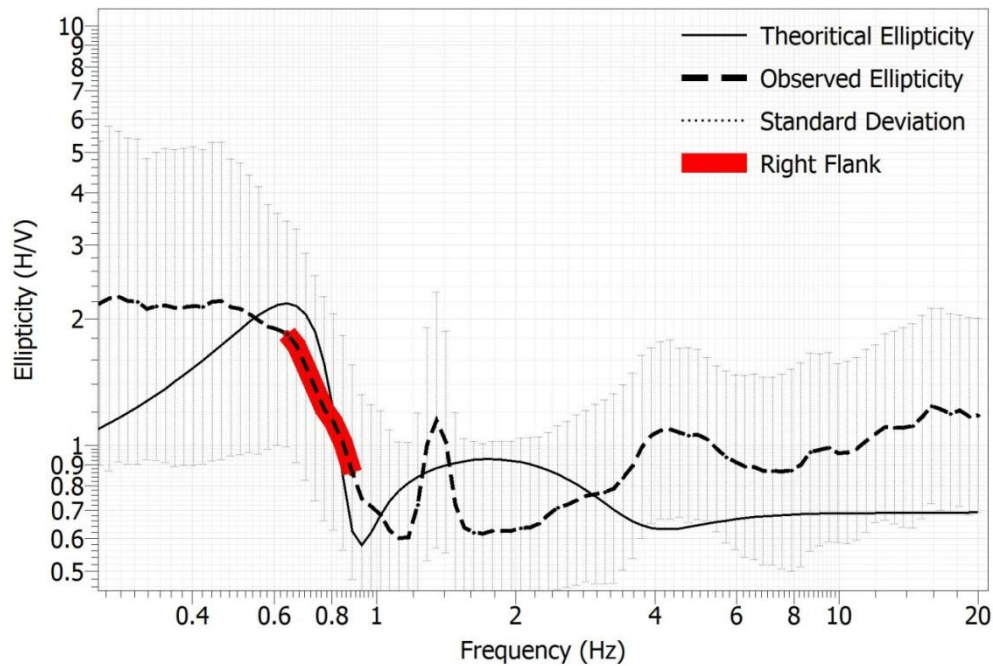
Fig. 6 Theoretical and observed ellipticity curves for HRM array. Dash and thin black lines present observed Ellipticity and calculated Ellipticity respectively. Also thick red line in right flank of observed Ellipticity curves which is used in inversion process
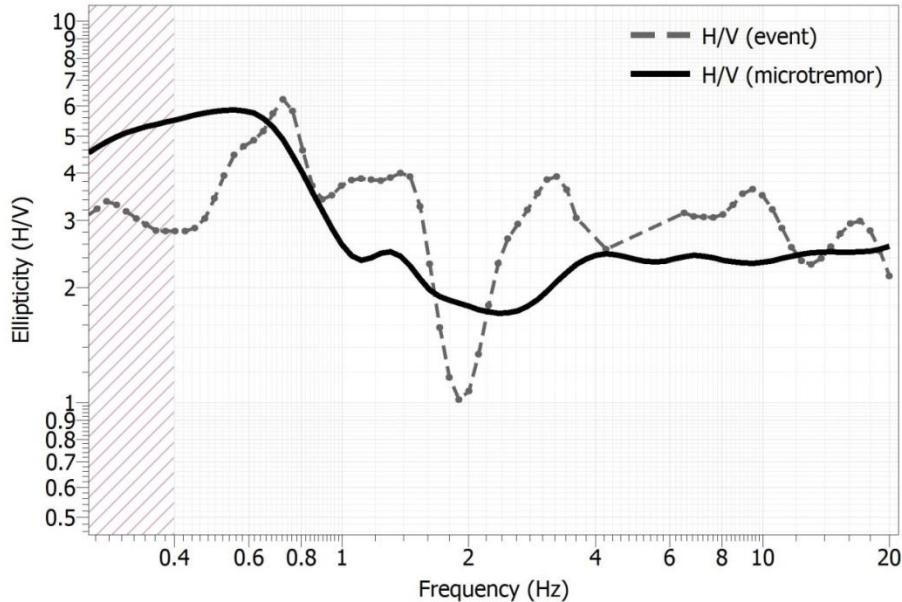

Fig. 7 This figure shows horizontal to vertical spectral ratio (HVSR) curves for HRM array. Dash and thick black lines present H/V of earthquake records and H/V of microtremor respectively. Dash lines at frequency lower than 0.4 Hz indicated that this part of earthquake data isn't reliable, because of time-history length (Tmax = Length/10)

3.4. Step 4: joint inversion of dispersion curve, ellipticity and peak of HVSR

We use DINVER software for joint inversion of dispersion and ellipticity curves based on Conditional Neighborhood Algorithm [29, 30, and 31]. Two shallow layers down to 30 meters with known shear wave velocity between 300 to 500 m/s and 5 layers with variable thickness with allowable lower boundary depth, respectively 100, 200, 500, 1000 and 2000 meters with unknown shear wave velocity, changing from 400 to 3500

m/s, over a half space with shear velocity greater than 1500 m/s were defined as input parameterization (Table 1). Inversion process was performed for model 1 to 5 with same condition but only model 5 presented here in Fig. 8 and 9. Actually, increasing the number of layers raises reliability of inversion results. Dispersion and ellipticity curves plus peak frequency of HV curves were applied together in inversion processing to fulfill theoretical probability curves to minimum misfits as following.

$$misfit = \sqrt{\sum_{i=1}^{n} \frac{(c_{di} - c_{ci})^2}{n. \sigma_i^2}} \qquad (6)$$

Where c_{ci} and c_{di} is calculated and observed values respectively, σ_i is standard deviation and n is number of frequency division. Fig. 8 obtained with the consideration of only dispersion curve of smallest array (D = 100 m) as the fundamental mode, while in Fig. 9 the fundamental mode and higher mode are considered together in inversion of all dispersion curves. Theoretical and observed dispersion and ellipticity curves as well as shear wave velocity profile with least misfits were presented in inversion results.

Table 1 input parameterization for HRM array location. In this table 5 model are presented

DEPTH(m)		**HRM**				
Based on	Model	1	2	3	4	5
geotechnical data	0-10			200-400		
	10-30			300-600		
Estimated data	30- 100					400-3500
	30- 200				400-3500	400-3500
	30- 500	400-3500	400-3500	400-3500		400-3500
	30-1000			400-3500	400-3500	400-3500
	30-2000		400-3500	400-3500	400-3500	400-3500
	BED ROCK			1500-5000		

Joint Inversion of dispersion and ellipticity curves only for array with 100 m aperture
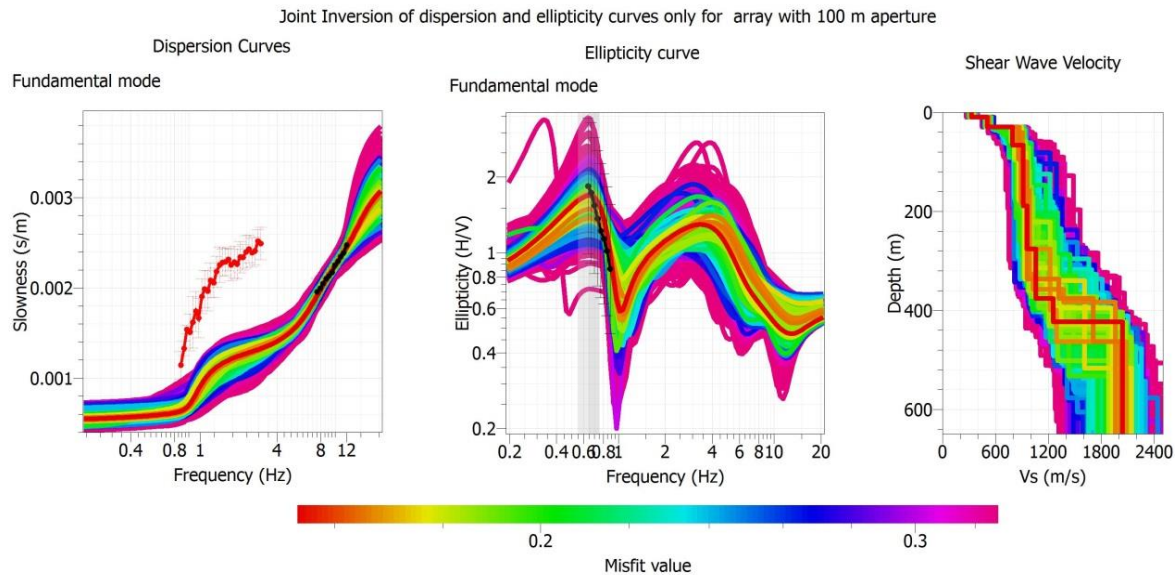
Fig. 8 Dispersion, Ellipticity and shear wave velocity profile curves. Here we considered only high frequency section of dispersion curve as fundamental mode. Red line in dispersion diagram is real fundamental extracted from larger array apertures (200, 400, 1000)
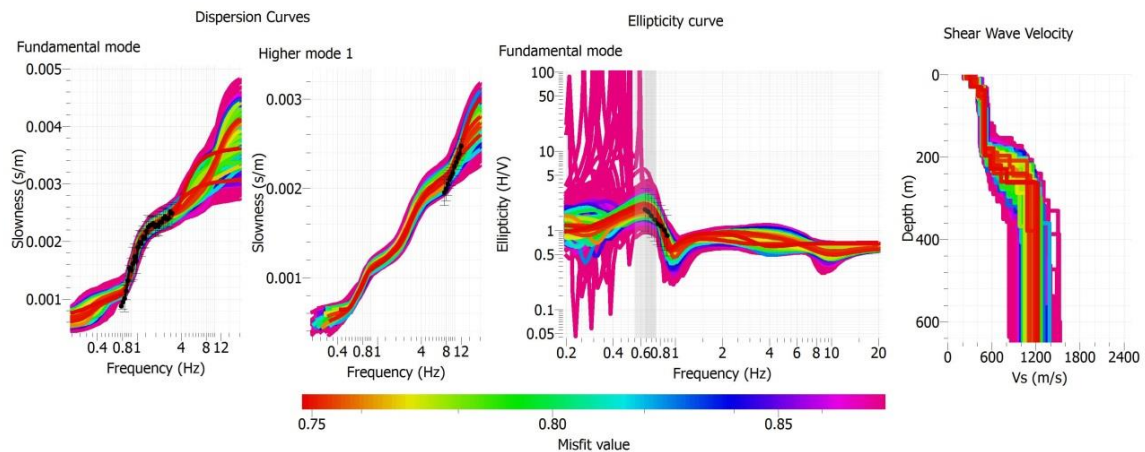
Fig. 9 Dispersion, Ellipticity and shear wave velocity profile curves. In this figure two modes 0 and 1 assumed in inversion processing across of part. Important effect of contributing higher modes clearly could be seen on shear velocity versus depth.

Fig. 10 shows theoretical dispersion curves for fundamental mode as well as modes 1, 2 and 3 resulted from back analysis of best model (minimum misfit, red profile in Fig. 9). As can be seen the three higher modes (1, 2 and 3) are near together and have a similar trend. Regarding this similarity the result of inversion assuming each one of these higher modes could not change the final shear wave velocity profile, significantly.
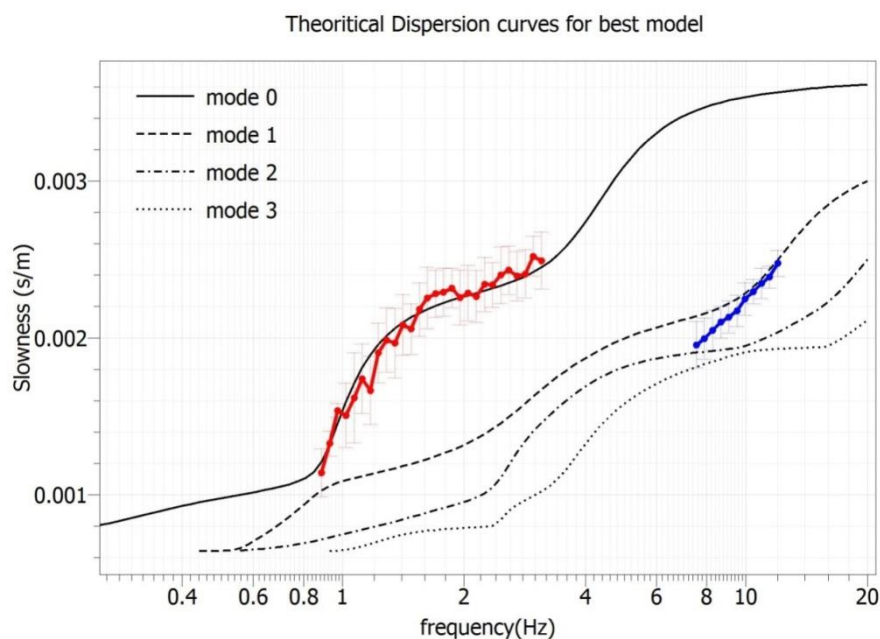

Fig. 10 Theoretical dispersion curves including fundamental and higher mode for best inverted model plus collective dispersion curves.

4. Discussion and Conclusion

In this study, 4 arrays with aperture 100 to 1000 meters were arranged to investigate shear wave velocity profile of deep sedimentary alluvium in south of Tehran near Imam Khomeini shrine (HRM station). As could be seen at Fig. 5, using array with aperture 100 meter, only 1 trend of phase velocity dispersion can be extracted. If we had only data of smallest array (D=100 meter), we usually performed inversion process with fundamental mode assumption for the obtained dispersion curve that result in

shear wave velocity profile including a layer with shear wave velocity equal to 900 to 1000 m/s at depths about 50 to 400 meters (Fig. 8).

Nowadays the small array measurement is a usual task in engineering seismology studies in urban area especially when there are not suitable places or when sufficient seismological equipment are not available to arrange large aperture array. As mentioned above this condition may results in wrong interpretations. Fortunately, for the present study we have 9 available velocimeters for each array and a vast agricultural land, which allows us to arranged large arrays (200, 400 and 1000 m aperture) measurements. Considering all the dispersion curves

derived from these larger arrays together, another trend of phase velocity can be observed clearly in lower frequencies and with lower velocity that could not be observed, using data of 100m array alone. Regarding the basic concepts of Rayleigh waves' propagation, it is more probable to consider this new trend as fundamental mode that means to consider the previous trend as higher mode. In addition, the trend of coherency observed in smallest array (D= 100m), identically recurred in larger arrays with aperture 200 and 400 meter, which confirm the effect of higher modes that cause a shift in the trend of dispersion curve at frequency greater than 4 Hz.

With this new idea and considering two parts of

dispersion curves as fundamental and mode one in inversion processing, a new shear wave velocity profile as Fig. 9 cab be obtained that shows one layer with velocity about 500 m/s between 50 to 250 meter.

Based on geological information of south of Tehran (see Ribben [32]) and the deepest geotechnical borehole, drilled by JICA (2001) [9], the studied area covered by fine grain silty-clayey alluvial deposits, belong to Kahrizak formation (Bs) with a thickness more than 200m; usually have low shear wave velocity. Thus, this new profile obtained by assumption the higher modes has better accordance with the geology of the studied area (Fig. 11).
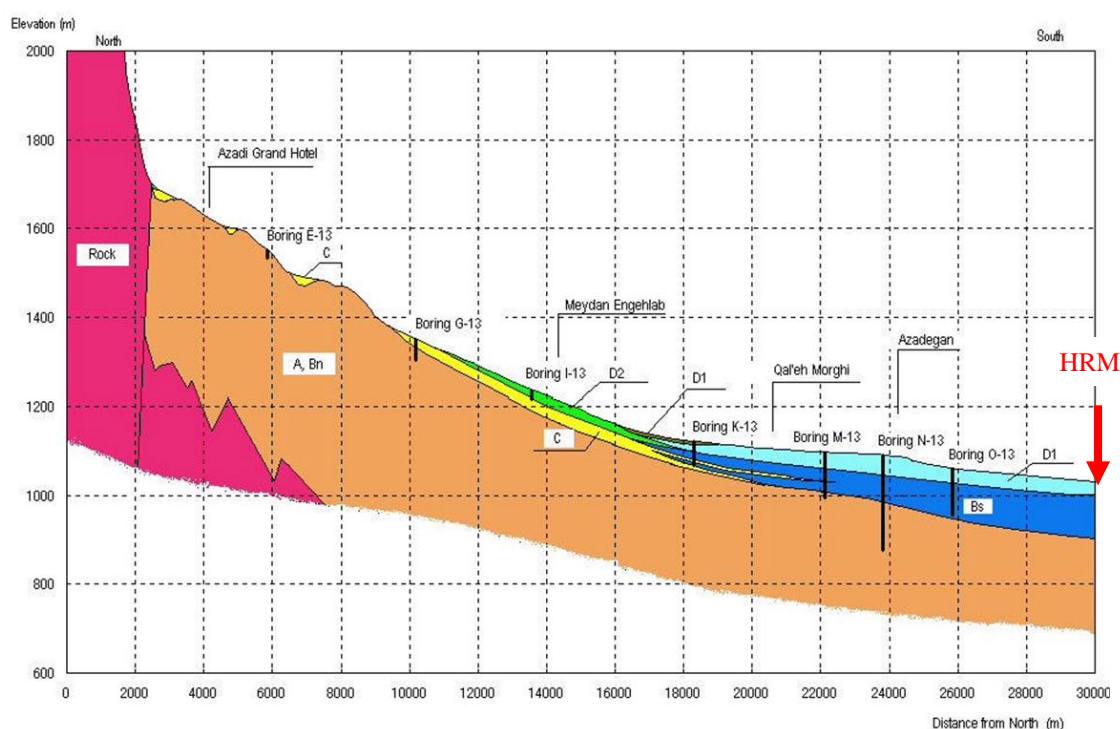

Fig. 11 geological section from north to south of Tehran (JICA, 2000). In HRM Location (red line at right of figure), two kinds of alluvium formation (Khahrizak on Upper red) could be seen at about depth of 200 meters.

This study shows that in region consisted of thick alluvial deposits like south of Tehran area, the employment of composite array with different aperture is necessary in order to check the real modes of observed dispersion curves and to extract real shear wave velocity in such deep layer substructures.

References

[1]   Davoodi M, Haghshenas E, Mirjalili M. Using ambient array method in evaluating the shear wave velocity profile of a site in Tehran, Journal of Seismology and Earthquake Engineering, Special Farsi Issue Winter, 2009.

[2]   Davoodi M, Haghshenas E, Esfahanizadeh M, Mirjalili M, Atashband S. Evaluate reliability of f-k and SPAC methods, 14th World Conference on Earthquake Engineering, 2008.

[3]   Shabani E, et al. Estimating shear-waves velocity structure by using array methods (FK and SPAC) and inversion of ellipticity curves at a site in south of Tehran, 14th World Conference on Earthquake Engineering, 2008.

[4]   Nourozi M. Application of Microtremor for Investigation of Sedimentary Basin Using Cross-Correlation Technique, M.Sc. thesis in IIEES, 2013.

[5] Mottaghi AA, Rezapour M, Tibuleac I. Ambient noise rayleigh wave shallow tomography in the Tehran region, Central Alborz, Iran, Seismological Research Letters, 2012, No. 3, Vol. 83, pp. 498-504.

[6] Shirzad T, Shomali H. Shallow crustal structures of the Tehran basin in Iran resolved by ambient noise tomography, Geophysical Journal International, 2014, Vol. 196, pp. 1162-1176.

[7] Fazlavi M, Haghshenas E, Cornou C, Bard PY. Determination of deep shear wave velocity profiles along north-south of Tehran (Iran) using join inversion of ellipticity and dispersion curves, (submitted for publication Bulletin of Earthquake Engineering in 2014).

[8] Haghshenas E, Fazlavi M. Deep subsurface shear wave velocity investigation in south of Tehran, using large aperture ambient noise array measurement, 15 World Conference on Earthquake Engineering, 2012, article 1117.

[9] JICA (Japan International Cooperation Agency) & CEST (Centre for Earthquake & Environmental Studies of Tehran, Tehran Municipality), The Study on Seismic Microzoning of the Greater Tehran Area in The Islamic Republic of Iran, Final report, 2000.

[10] SESAME group, Report on simulation for real sites – WP10 Set of noise synthetics for H/V and array studies from simulation of real sites and comparison for test sites, SESAME Deliverable D11.10 & D17.10, 2004a, available at http://sesame-fp5.obs.ujf-grenoble.fr/Deliverables/Del_D11-D17.pdf.

[11] Tokimatsu K. Geotechnical site characterization using surface waves, Earthquake Geotechnical Engineering, 1997, pp. 1333-1368.

[12] Lacoss RT, Kelly EJ, Toksoz MN. Estimation of seismic noise structure using arrays, Geophysics, 1969, Vol. 34, pp. 21-38.

[13] Capon J. High- resolution frequency- wavenumber spectrum analysis, Proceedings of the IEEE, 1969, No. 8, Vol. 57, pp. 1408-1418.

[14] Asten MW, Henstridge J. Array Estimators and the Use of Microseisms for Reconnaissance of Sedimentary Basins, 1984.

[15] Okada H. The microtremor survey method, exploration geophysics, Geophysical monographs series, 2004, Vol. 12.

[16] Aki K. Space and time spectra of stationary stochastic waves, with special reference to microtremors, Bulletin of the Earthquake Research Institute, 1957, Vol. 35, pp. 415-456.

[17] Henstridge J. A signal processing method for circular arrays, GEOPHYSICS, 1979, No. 2, Vol. 44, pp. 179-184.

[18] Bettig B, Bard PY, Scherbaum F, Riepl J, Cotton F, Cornou C, Hatzfeld D. Analysis of dense array noise measurements using the modified spatial auto-correlation method (SPAC) application to the Grenoble area, Bolletino di Geosica Teoricaed Applicata, 2001, Vol. 42, pp. 281-304.

[19] Nakamura Y. A Method for Dynamic Characteristics Estimation of Subsurface Using Microtremor on the Ground Surface, 1989.

[20] Bard PY. Microtremor measurements: A tool for site effect estimation?, Proceeding of the Second International Symposium on the Effects of Surface Geology on Seismic Motion, Yokohama, Japan, 1998, Vol. 3, pp. 1251-1279.

[21] Bonnefoy-Claudet S, Cornou C, Bard PY, Cotton F, Moczo P, Kristek J, Fäh D, H/V ratio: a tool for site effects evaluation, Results from 1D noise simulations, Geophysical Journal International, 2006b, Vol. 167, pp. 827-837.

[22] Haghshenas E, Bard PY, Theodulidis N. SESAME WP04 Team, Empirical evaluation of microtremor H/V spectral ratio, Bulletin of Earthquake Engineering, 2008, No. 1, Vol. 6, pp. 75-108.

[23] Najafizadeh J, Kamalian M, Jafari M, Khaji N. Seismic analysis of rectangular alluvial valleys subjected to incident sv waves by using the spectral finite element method, IJCE, 2014, No. 3, Vol. 12, pp. 251-263.

[24] SESAME group, Report of the WP04 – H/V technique: Empirical evaluation Comparison of experimentally and theoretically estimated transfer functions with the (H/V) spectral ratio and evaluation of the applicability of the latter in cases of linear or/and non-linear soil behaviour, SESAME Deliverable D16.04, 2004b; available at http://sesame-fp5.obs.ujf-grenoble.fr/Deliverables/D16-04.pdf.

[25] Haghshenas E. Geotechnical condition and local seismic hazard in Tehran, PhD Thesis, Joseph Fourier University, Grenoble-I (18/07/2005), 2005.

[26] ISMN (Iran Strong Motion Network), annual report and catalogues, http://BHRC.ac.ir.

[27] Hobiger M, Cornou C, Wathelet M, Di Giulio G, Knapmeyer-Endrun B, Renalier F, Bard PY, Savvaidis A, Hailemikael S, Le Bihan N, Ohrnberger M, Theodoulidis N. Ground structure imaging by inversions of Rayleigh wave ellipticity: sensitivity analysis and application to European strong-motion sites, Geophysical Journal International, 2013, No. 1, Vol. 192, pp. 207-229.

[28] NERIES (NEtwork of Research Infrastructures for European Seismology), Using Ellipticity Information for Site Characterisation, JRA4, 2010

[29] Sambridge M. Geophysical inversion with a neighbourhood algorithm, Geophysical Journal International, 1999, Vol. 138, I: 479-494 & II: 727-746.

[30] Wathelet M, Jongmans D, Ohrnberger M. Direct inversion of spatial autocorrelation curves with the neighborhood algorithm, Bulletin of the Seismological Society of America, 2005, No. 5, Vol. 95, pp. 1787-1800.

[31] Wathelet M. An improved neighborhood algorithm, parameter conditions and dynamic scaling, Geophysical Research Letters, 2008, Vol. 35.

[32] Ribben EH. Geological observations on alluvial deposits in northern Iran, Geological Survey of Iran, 1966, Vol. 9.